# Phosphonocarboxylates inhibit the second geranylgeranyl addition by Rab Geranylgeranyl Transferase

**Rudi A. Baron[1*], Richard Tavaré[1§], Ana C. Figueiredo[1], Katarzyna Błażewska[2], Boris A. Kashemirov[2], Charles E. McKenna[2], Frank H. Ebetino[3], Adam Taylor[4], Michael J. Rogers[4], Fraser P. Coxon[4], and Miguel C. Seabra[1,5,6¶]**

*[1] Molecular Medicine, National Heart and Lung Institute, Imperial College London, London SW7 2AZ, UK, [2] Department of Chemistry, University of Southern California, Los Angeles, California 90089-0744, [3] Procter & Gamble Pharmaceuticals, Cincinnati, Ohio, USA, [4] Bone & Musculoskeletal Programme, Institute of Medical Sciences, University of Aberdeen, Aberdeen, AB25 2ZD, UK, [5]Instituto Gulbenkian de Ciência, 2780-156 Oeiras, Portugal, [6]Faculdade de Ciências Médicas, Universidade Nova de Lisboa, 1169-056 Lisboa, Portugal*

[*] Present address: Cerenis Therapeutics, 31682 Labège, France

[§] Present address: Kings College London, Division of Imaging sciences, The Rayne Institute, 4th floor, Lambeth Wing, St. Thomas Hospital, London SE1 7EH

[¶]Address correspondence to Miguel C. Seabra: email: m.seabra@imperial.ac.uk

Running title: Mechanism of RGGT inhibition by bisphosphonates

**Rab geranylgeranyl transferase (RGGT) catalyzes the post-translational geranylgeranyl (GG) modification of (usually) two C-terminal cysteines in Rab GTPases. Here we studied the mechanism of the Rab geranylgeranylation reaction by bisphosphonate analogs in which one phosphonate group is replaced by a carboxylate (phosphonocarboxylate, PC). The phosphonocarboxylates used were 3-PEHPC, which was previously reported, and (+)-3-IPEHPC, a >25-fold more potent related compound as measured by both $IC_{50}$ and $K_i$. (+)-3-IPEHPC behaves as a mixed-type inhibitor with respect to GG pyrophosphate (GGPP) and an uncompetitive inhibitor with respect to Rab substrates. We propose that phosphonocarboxylates prevent only the second GG transfer onto Rabs based on the following evidence. First, geranylgeranylation of Rab proteins ending with a single cysteine motif such as CaaX, is not affected by the inhibitors, either *in vitro* or *in vivo*. Second, the addition of an -aaX sequence onto Rab-CC proteins protects the substrate from inhibition by the inhibitors. Third, we demonstrate directly that in the presence of (+)-3-IPEHPC, Rab-CC and Rab-CXC proteins are modified by only a single GG addition. The presence of (+)-3-IPEHPC resulted in a preference for the Rab N-terminal cysteine to be modified first, suggesting an order of cysteine geranylgeranylation in RGGT catalysis. Our results further suggest that the inhibitor binds to a site distinct from the GGPP-binding site on RGGT. We suggest that phosphonocarboxylate inhibitors bind to a GG-cysteine binding site adjacent to the active site, which is necessary to align the monoGG-Rab for the second GG addition. These inhibitors may represent a novel therapeutic approach in Rab-mediated diseases.**

Most proteins of the Ras-like GTPase superfamily need to be post-translationally modified by prenyl groups in order to associate with cellular membranes and to activate downstream effectors (1). Protein prenylation involves the formation of a thioether link between conserved C-terminal cysteines in

protein substrates and farnesyl pyrophosphate (FPP) or geranylgeranyl pyrophosphate (GGPP) (2,3). These prenyl pyrophosphates, which originate from the mevalonate pathway are utilized by three different prenyltransferase enzymes (2,3). Farnesyl transferase (FT) and Geranylgeranyl transferase type I (GGT-I) transfer FPP or GGPP, respectively, to a cysteine residue in the context of a C-terminal CaaX motif, where C is a cysteine, a is an aliphatic residue and X is any amino acid. X contributes significantly to substrate specificity in FT and GGT-I (2). Rab geranylgeranyl transferase (RGGT) is distinct from FT and GGT-I in that it specifically recognizes Rab proteins, which vary in their C-terminus containing CCXX, XCXC, XXCC, CCXXX, CaaX and other motifs (3). RGGT exhibits exquisite specificity for Rabs due to the strict requirement of Rab Escort Protein (REP), which is a general Rab-GDP binding protein (4). RGGT is a heterodimeric enzyme consisting of a 60 kDa α-subunit and a 38 kDa β-subunit, and shares 30% homology with its FT and GGT-I counterparts (5). The α-subunit associates with REP in a very small area compared to the entire surface occupied by the complex, while the β-subunit binds one molecule of GGPP in a large hydrophobic cavity (5,6).

Although a large number of specific FT and GGT-I inhibitors have been developed as potential anti-cancer agents (7,8), few inhibitors of RGGT exist. Recently the phosphonocarboxylate 3-PEHPC, was identified as a specific RGGT inhibitor, thereby selectively preventing the prenylation of Rab proteins in cells (9,10). This compound was derived from the bisphosphonate (BP), risedronate, which is used clinically in the treatment of osteoporosis, due to its ability to potently inhibit the activity of bone-resorbing osteoclasts (11). Although BPs such as risedronate prevent Rab prenylation, they do not act by inhibiting RGGT. Rather, these drugs prevent the synthesis of FPP and GGPP by inhibiting FPP synthase, thereby preventing all protein prenylation (12). 3-PEHPC is a weak RGGT inhibitor and consequently a weak inhibitor of bone resorption. However, we have recently identified a similar phosphonocarboxylate, (+)-3-IPEHPC, which is at least 25 times more potent than 3-PEHPC as an inhibitor of RGGT. Here, we report the surprising finding that phosphonocarboxylate inhibitors of RGGT act by inhibiting only the second Rab geranylgeranylation event, therefore providing specificity towards Rab proteins with a double cysteine C-terminal motif.

**Experimental procedures**

*Plasmid constructs* – Human REP1 cDNA was cloned into pFastBacHTb and produced as described previously (13). Rat RGGT was prepared as described previously (13). Canine Rab1a, human Rab27a, human Rab5a, human Rab18, human Rab6a were amplified by PCR and cloned into pET14b and human Rab13 and mouse Rab23 were cloned into pGEX-4T-1 as described previously (14). The indicated C-terminal sequence mutants were obtained by using the Quickchange mutagenesis kit (Stratagene). The sequences of all plasmid constructs used were confirmed by DNA sequencing.

*Recombinant Proteins* - The recombinant proteins RGGT and REP1 were prepared by infection of Sf9 cells with recombinant baculoviruses encoding each subunit of the desired enzyme and purified by nickel Sepharose-affinity chromatography as described previously (13,15). Recombinant 6xHis and GST-tagged Rab proteins were purified by nickel sepharose or glutathione sepharose affinity as described previously (16,17). All recombinant proteins were snap frozen in small aliquots and stored at - 80°C until use.

*Bisphosphonates* - 2-Hydroxy-2-phosphono-3-pyridin-3-yl-propionic acid (3-PEHPC, previously referred to as NE-10790) [1] was a gift from Procter & Gamble Pharmaceuticals. 2-Hydroxy-3-imidazo[1,2-a]pyridin-3-yl-2-phosphonopropionic acid (3-IPEHPC) [2] was synthesized and resolved into its component enantiomers by methods reported elsewhere (McKenna et al., manuscript in preparation).The (+)-enantiomer was used in the present study, since this has been shown to be selective towards RGGT, and a more potent inhibitor of this enzyme than the (-)-enantiomer (McKenna et al., manuscript in preparation). The enantiopurity was determined to be > 98 % by

chiral HPLC using a Prontosil AX QN (eluted isocratically with 0.7 M TEAA buffer containing 75 % MeOH at pH 5.8; UV detection at 265 nm, flow rate 3 ml/min). The more active (+)-enantiomer elutes first. The specific optical rotation $[\alpha]_D^{25}$ +109 ° was measured on a Jasco J100 Polarimeter.

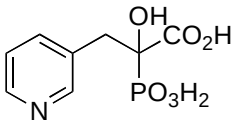


**1**, 3-PEHPC

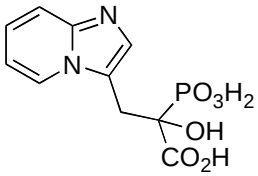


**2**, 3-IPEHPC

*In vitro prenylation assay* - RGGT activity was measured by determining the amount of [$^3$H] GGPP transferred to Rab proteins (15,18). Unless otherwise indicated, the standard reaction mixture contained the following concentrations in a final volume of 25µl: 50mM sodium HEPES (pH 7.2), 5mM $MgCl_2$, 1mM Nonidet P-40, 1mM dithioerythritol (DTE), 5µM [$^3$H] GGPP (specific activity = 800 dpm/pmole), 4µM Rab proteins, 2µM REP1 and 50nM RGGT. After 20 min at 37°C, the reaction was stopped by addition of 1ml of Ethanol/HCl (9:1) and the incorporated radioactivity was measured by filtration on glass fiber followed by scintillation counting (18).

*Kinetic Analyses* - For the inhibition pattern experiments with biphosphonate compounds, data were collected for times where product accumulation was linear. The observed initial velocity data were fitted to equation 1 for mixed-type inhibition, where $K_m$ is the Michaelis constant for the varied substrate S, and $K_i$ is the mixed-type inhibition constant for (+)-3-IPEHPC and 3-PEHPC.

$$\frac{1}{v} = \frac{K_m}{V_{max}}\left(1 + \frac{[I]}{K_i}\right)\frac{1}{[S]} + \frac{1}{V_{max}}\left(1 + \frac{[I]}{\alpha K_i}\right)$$

For uncompetitive inhibition the observed initial velocity data were fitted to equation 2.

$$\frac{1}{v} = \frac{K_m}{V_{max}}\frac{1}{[S]} + \frac{1}{V_{max}}\left(1 + \frac{[I]}{K_i}\right)$$

The $K_i$ and associated SEM for (+)-3-IPEHPC and 3-PEHPC were calculated using shared parameter curve fitting for all inhibitor concentrations using the average of duplicate determinations. The error represents the divergence between fitted curves.

*Proteolytic digestion of prenylated Rab proteins and peptide analysis* - The peptides were prepared essentially as described previously (19,20). The RGGT mixture (25µl), 2µM REP1, 50nM RGGT, 5µM Rab proteins, 5µM GGPP (specific activity = 1600 dpm/pmole) was precipitated by addition of cold acetone (1ml) for 1h at 4°C. The pellet was washed with 1ml of cold acetone and resuspended in 100µl of 25mM Tris-HCl (pH 8), 4% CHAPS, 1mM EDTA and 3µg of endoproteinase C-Lys (Boehringer Mannheim) and incubated overnight at 37°C. The resulting peptides were isolated on a reverse-phase µRPC C2/C18 SC 2.1/10 column (Pharmacia) using a SMART System chromatography instrument (Pharmacia). The column was equilibrated in MilliQ water with 0.06% trifluoroacetic acid (TFA) at room temperature at a flow rate of 200µl/min. 50µl of sample were injected and the peptides were separated by a 3.5ml linear gradient (0-70% acetonitrile) and 2.5ml of 100% acetonitrile (0.056% TFA). The radioactivity in each fraction (200µl) was measured by scintillation counting (Beckman LS 6000SC).

*[3H]GGPP binding to RGGT* – The reaction mixture (25µl), 2µM REP1, 100nM RGGT, 4µM Rab proteins, 2µM [$^3$H]GGPP (specific activity = 4500 dpm/pmole), 100µM (+)-3-IPEHPC was incubated for 20min at 37°C and was mixed with 2µl of rabbit anti-RGGT (H492) plus 25µl of protein G beads (GE healthcare). The solution was gently shaken for 2h at 4°C. The beads were washed 4 times with 1ml of PBS and the proteins were precipitated by adding 200µl of EtOH:HCl (9:1). The samples were centrifuged at 20,000 x g for 10min and the radioactivity in 200µl of supernatant was determined by scintillation counting.

*Analysis of prenylation of GFP-Rabs in 293 cells* – Human Embryonic Kidney 293 (293) cells were grown in DMEM medium supplemented with 10% FCS and seeded into 12-well plates at $2x10^5$ cells/well. The following day, cells were transfected with 400ng of purified plasmids (the EGFP-Rab constructs

detailed above) using Fugene6 transfection reagent, according to the manufacturer's instructions (Roche). Immediately after transfection, 0-1.5 mM 3-PEHPC, was added to the culture medium and cells incubated for 24H. Cells were then lysed in Triton X-114 fractionation buffer, and prenylated Rabs separated from unprenylated Rabs as previously described (9). 30μg of fractionated lysates (aqueous and detergent-rich phases, containing unprenylated and prenylated Rabs, respectively) were electrophoresed on 12% polyacrylamide Criterion gels (Bio-Rad), transferred to PVDF membrane, then western blotted for GFP-Rabs using an anti-GFP antibody and also β-actin as a loading control (Sigma). Bands were visualized following hybridization with secondary antibodies conjugated to AlexaFluor-680 and AlexaFluor-800 using an Odyssey infra-red imaging system (LiCor).

*Analysis of localization of GFP-Rabs in 293 cells* - 293 cells were seeded onto 9 mm glass coverslips in 48 well plates at $4x10^4$ cells/well, then transfected the following day with 100ng of EGFP-Rab constructs using Fugene6. In some cases, cells were also incubated with 1mM 3-PEHPC. Cells were incubated for 24H, then fixed in 4% formaldehyde. Nuclei were counterstained with TO-PRO-3 iodide and the cells were examined using a Zeiss LSM510 META confocal microscope after mounting the coverslips onto glass slides.

*Icmt assay* - Enriched Icmt membranes were a kind gift of Patrick J. Casey (Department of Pharmacology, Duke University). The methylation of Rab1a was measured after *in vitro* prenylation of the protein. The final volume on prenylation reaction (25μl) contains: 50mM sodium HEPES (pH 7.2), 5mM $MgCl_2$, 1mM DTE, 20μM cold GGPP, 10μM Rab1a proteins, 2μM REP1, 100nM RGGT and 100μM (+)-3-IPEHPC. After 30 min at 37°C, 5μl of buffer 50mM sodium HEPES (pH 7.2), 5mM $MgCl_2$, 1mM DTE, 10μM [$^3$H] S-adenosyl methionine (specific activity = 650 dpm/pmol) and 1 μg of enriched Icmt membranes were added for 40 min. The reaction was stopped and treated as described previously.

**Results**

*PCs are mixed-type inhibitors of RGGT.* We previously reported weak RGGT inhibition by a racemic phosphonocarboxylate compound, 3-PEHPC (10). The pyridine cycle of this compound was replaced by an imidazo[1,2-α]pyridine cycle to create (+)-3-IPEHPC, a PC analogue of the BP, minodronate. We found that (+)-3-IPEHPC was 25-fold more potent for RGGT inhibition compared to 3-PEHPC using Rab1a as the substrate ($IC50_{(+)\text{-}3\text{-}IPEHPC}$ = 1.3 ± 0.22 μM; $IC50_{3\text{-}PEHPC}$ = 31.9 ± 2.1 μM; Table 1 and Figure 1). To assess the inhibition type with respect to both substrates, Rab and GGPP, we designed kinetic experiments using (+)-3-IPEHPC. Double-reciprocal plots obtained from such experiments are shown in Figure 2A for Rab and Figure 2B for GGPP. Equations describing competitive, noncompetitive, uncompetitive and mixed-type inhibitions were fitted to the data for Rab1a, resulting in a best fit for an uncompetitive inhibition (Figure 2A); the calculated $K_i$ under the conditions employed in this assay was 0.21 ± 0.09 μM. Similar analysis for the lipid substrate, GGPP, suggests a mixed-type inhibition, ie, the inhibitor behaves both as competitive and noncompetitive inhibitor (Figure 2B); we calculated that $K_i$ = 0.074 ± 0.029 μM. Interestingly, 3-PEHPC gave a similar type of inhibition for both substrates with $K_i$ values of 5 ± 0.18 μM and 33.6 ± 11.1 μM for GGPP and Rab1a substrates respectively (Table 2).

*Inhibition of Rab prenylation by PCs is dependent on the C-terminal prenylation motif.* The velocity of the prenylation reaction can be described as $v_t = v_1 * v_2$, where $v_t$ is the total velocity of the reaction and $v_1$ and $v_2$ the velocities for the addition of the first and the second GGPP, respectively. To assess the possibility that different forms of the enzyme/substrate complex are unequally sensitive to (+)-3-IPEHPC, we measured $IC_{50}$ values for Rab1a substrates with different C-terminal motifs. To generate mono-prenylated or di-prenylated products at different C-terminal positions, the –CC motif of Rab1a was replaced by CSC, CCS, CS, or SC, and the respective recombinant proteins were produced as His

tagged fusion proteins in *E. coli* and purified. *In vitro* prenylation assays were then performed with those substrates at different inhibitor concentrations (Table 1). The $IC_{50s}$ generated for Rab1a-CC, Rab1a-CSC and Rab1a-CCS proteins were very similar, at around 1 μM. This result suggests that different double-cysteine motifs in the context of the same Rab does not affect significantly the inhibition by (+)-3-IPEHPC. Conversely, the $IC_{50}$ varied with the Rab substrate used. Comparing different Rab proteins containing double cysteine motifs, Rab1a (CC), Rab5a (CCSN), Rab6a (CSC) and Rab27a (CGC), we observed a 30-fold higher $IC_{50}$ for Rab6 as compared with Rab1a, Rab5a and Rab27a (Table 1). Similar differences were found when we measured $IC_{50}$ values for 3-PEHPC, which was 50-fold higher for Rab6 substrate compared to Rab27a.

We next determined whether other factors in the C-terminal motif affected the inhibitory properties of PCs. In the context of Rab5a (CCSN), changing to –CCQNI (present in Rab11a), resulted in an increase in $IC_{50}$ from 0.4 μM to 16.5 μM for (+)-3-IPEHPC (Table 1), whereas when the motif was changed to CCVLL, the $IC_{50}$ was increased to a lesser extent ($IC_{50}$ = 5.9 μM) (Table 1). Similar differences were found using (+)-3-PEHPC as the inhibitor (Table 1). Both C-terminally modified Rab5 proteins were doubly-geranylgeranylated as verified by chromatography as described below (data not shown). The spatial alignment of the CCVLL and the CCQNI sequences showed high similarity in terms of surface area and length, but the CCQNI sequence was much more hydrophilic than CCVLL (the grand average of hydropathy coefficients or GRAVY are 0.5 and 3.36, respectively). Therefore, the length and the polarity of the C-terminal prenylation motif is an important factor in influencing the inhibitory properties of PCs.

Surprisingly, (+)-3-IPEHPC no longer behaved as an inhibitor when single-cysteine Rabs were used in the assay. We studied three wild type proteins, Rab13 (CSLG, as a GST fusion), Rab18 (CSVL, as a GST fusion) and Rab23 (CSVP), and in all three cases no significant inhibition was obtained with (+)-3-IPEHPC concentrations of up to 800 μM (Table 1). Consistently, both Rab5a (Rab5aCVLL) and Rab27a (Rab27aCVLL) single-cysteine mutants showed the same pattern (Table 1). Furthermore, Rab1a mutants with a single prenylatable cysteine (Rab1a-CS and Rab1a-SC) exhibited a 100-fold increase in $IC_{50}$ values for (+)-3-IPEHPC when used as substrates (221 ± 11 and 187 ± 8 μM, respectively) as compared to the wild-type Rab1a-CC (Table 1). These results indicate that the C-terminal sequence of the Rab substrates plays a critical role in determining susceptibility to inhibition by PCs, with the mono-geranylgeranylated (mono-GG) Rab proteins unaffected, or only partially affected by the compound, and suggest that the first event of prenylation ($v_1$) is not affected by the inhibitor. This model could also explain why (+)-3-IPEHPC behaved as a mixed-type inhibitor. The compound may act differently for each prenylation reaction, $v_1$ and $v_2$, i.e., the different transition states for single and double prenylation.

*PCs inhibit only the second event of prenylation*. To test our hypothesis that only the second prenylation event is inhibited by (+)-3-IPEHPC, we developed a chromatographic method to discriminate between mono-geranylgeranylated and di-geranylgeranylated forms of Rab proteins. Initially, we defined the elution volumes of mono-geranylgeranylated and di-geranylgeranylated peptides. We subjected Rab1a-CC, Rab1a-CS and Rab1a-SC to *in vitro* prenylation and the products of the reaction were digested by Endoproteinase C-Lys. The peptides obtained were separated on a C2/C18 reverse phase column with an acetonitrile/water gradient and the elution of [$^3$H] GGPP-labelled fractions were analyzed (Figure 3). Under the conditions of the experiment, a clear separation was achieved between mono- and di-geranylgeranylated peptides. Rab1a-CC digestion profile showed a single peak eluting at 95% acetonitrile (fraction 24) whereas the Rab1a-CS and SC peptides eluted as a single peak at 75% acetonitrile (fraction 18) (Figure 3). Then, we performed *in vitro* prenylation reactions with Rab1a-CC in presence or absence of (+)-3-IPEHPC at a saturating concentration (100μM). Strikingly, in the presence of (+)-3-IPEHPC, the di-geranylgeranylated peak disappeared, while a peak corresponding to

mono-geranylgeranylated peptide appeared (Figure 3). Moreover, an identical profile was obtained when Rab1a-CSC or Rab5 (CCSN) were used as substrates, as well as when the proteins were digested with trypsin instead of endoproteinase C-Lys (data not shown). Furthermore, we detected mono-GG proteins when RGGT was treated with 3-PEHPC, similar to the results obtained with (+)-3-IPEHPC (data not shown). These results clearly indicate that only the second prenylation event is inhibited by PC compounds, and that the C-terminal ending of Rab proteins is a critical determinant of susceptibility to inhibition.

*(+)-3-IPEHPC does not preclude GGPP binding to RGGT*. Based on the competition experiments, the inhibitor should not compete for substrate binding to RGGT, or only partially in case of GGPP. To assess the association of GGPP with the enzyme, we performed *in vitro* prenylation assays with or without (+)-3-IPEHPC. Then, we analyzed GGPP molecules associated with RGGT by immunoprecipitation of the enzyme using protein-G beads coupled to rabbit anti-RGGT antibody. Excess GGPP was removed by extensive washing of the beads. The RGGT-bound GGPP was then separated from Rab-GG by methanol extraction as Rab-GG precipitates under these conditions. In the absence of inhibitor, RGGT-bound GGPP was isolated when no Rab substrate was added, consistent with the existence of a stable GGPP binding site (Figure 4). As the yield of enzyme after immunoprecipitation is approximately 50%, approximately 80% of RGGT was loaded with radiolabeled GGPP under these conditions (Figure 4). This RGGT-bound GGPP disappeared in the presence of Rab1a-CC, but not in the presence of Rab1a-CS (Figure 4). These results suggested that the inability to doubly-geranylgeranylate Rab1a-CS led GGPP to remain stuck in the GGPP binding site. The inhibitor did not compete for the RGGT-bound GGPP in the absence of Rab protein, or in the presence of Rab1a-CS, indicating that it does not preclude the binding of GGPP to RGGT (Figure 4). These results strongly suggest that the inhibitor binds to a site that is distinct from the GGPP-binding site on RGGT. Interestingly, when inhibitor and Rab1a-CC were both incubated with the enzyme, RGGT-bound GGPP could now be elicited (Figure 4). This result suggests that the presence of inhibitor with Rab1a-CC leads to freezing of GGPP on the RGGT-binding site, as when Rab1a-CS is present (in the absence of inhibitor). In both cases, the presence of GGPP stuck on RGGT may reflect an inhibition of GG transfer due to an inability of the monoprenylated Rab protein to move to a second site on RGGT, which accepts a newly transferred GG-cysteine.

*Prenylation and localization of doubly-prenylated Rab proteins is disrupted by PCs in 293 cells.* To assess whether the susceptibility of Rabs with different C-terminal motifs to inhibition by PCs in intact cells matched the *in vitro* assays, we transfected 293 cells with GFP-Rab constructs (Rab1A, Rab5, Rab6, and Rab18) and analyzed the ability of 3-PEHPC to inhibit prenylation *in vivo* and disrupt the localization of these Rab proteins (Figure 5). Accordingly, we found that prenylation of GFP-Rab1a, GFP-Rab5a and GFP-Rab6a was susceptible to inhibition by 3-PEHPC, as evidenced by their significant shift from the detergent phase (prenylated forms) to the aqueous phase (unprenylated form) upon Triton X-114 partitioning of cell lysates (Figure 5A). In this experiment, the over-expression leads to the presence of a proportion of EGF-Rab in the aqueous phase even at steady-state. Moreover, 1 mM 3-PEHPC completely prevented the specific membrane targeting of Rab1a, Rab6a and Rab5a, resulting in a diffuse cytoplasmic localization of these Rabs (Figure 5B), without affecting the growth or viability of the cells over this culture period (data not shown). Reflecting the enzyme inhibition data, the order of potency for inhibition of prenylation by 3-PEHPC was Rab5a>Rab1a>Rab6. In contrast, both the prenylation and subcellular localization of the mono-prenylated, CaaX motif-containing Rab18, was resistant to 3-PEHPC treatment, in agreement with the enzyme assays. Furthermore, despite containing a CaaX motif, the prenylation and subcellular localization of Rab18 was also unaffected by GGTI-298, a specific inhibitor of GGT-I (data not shown).

*Order of prenyl addition on Rab proteins*. Two previous studies examined the order of GG addition by RGGT and proposed that the N-terminal cysteine is preferred to the C-terminal one (16,21). However the substrates used in those studies were single-cysteine mutants of Rab1a and a fluorescent derivative of GGPP, respectively, and not native substrates. Since PCs specifically block only the second event of prenylation, they are useful tools to characterize the first event of Rab prenylation. We took advantage of the fact that the Isoprenyl cysteine methyltransferase (Icmt) can only methylate the C-terminal geranylgeranylated cysteine in a CaaX or CXC motif and not in the context of a CC motif (14). Using a coupled prenylation/methylation assay in vitro, we observed as expected, methylation of the Rab1a-SC mutant but not of the Rab1a-CS mutant or wild type Rab1a-CC (Figure 6), which is consistent with double prenylation of the CC motif, as previously reported (14). Furthermore, the Rab1a-SC mutant was methylated by Icmt in the presence or absence of inhibitor, confirming the recognition of this motif by the methyltransferase and validating the experimental approach. Note that the inhibitor concentration used in the experiment (100 μM) was below the $IC_{50}$ for Rab1a-CS or SC mutants and therefore would have had little effect on the prenylation reaction. Treatment with (+)-3-IPEHPC did not lead to increased methylation of Rab1a-CC, indicating that prenylation of the N-terminal cysteine is not affected by the inhibitor. Furthermore, when the Rab1a-CSC mutant was treated with 3-IPEHPC, we observed a dramatic reduction in methylation compared to untreated reaction, indicating that prenylation of the C-terminal cysteine is inhibited by 3-IPEHPC, i.e., this is the second prenylation step. Similar experiments with wild type Rab27a (CGC) showed identical results (data not shown). These results demonstrate that the N-terminal cysteine in dual-prenylated Rabs is preferred for the first GG addition.

## Discussion

We report here a mechanism of action for inhibition of RGGT by PCs. Our data suggests that these inhibitors act as partial inhibitors of the geranylgeranylation reaction, effectively inhibiting only the second GG addition onto those Rab substrates that contain double cysteine motifs at their C-terminus. Yet, these behave as effective inhibitors in cell studies presumably for two reasons. One is that the majority of Rabs are doubly-geranylgeranylated and the second is that the enzyme exhibits highest affinity for mono-prenylated intermediates in the reaction (16), raising the possibility that these inhibitors sequester the cellular pools of the enzyme in non-productive complexes. Additionally, mono-geranylgeranylation of normally di-geranylgeranylated Rabs, such as Rab5, leads to mistargeting to the endoplasmic reticulum, and loss-of-function (17). Therefore, even if a proportion of inhibitor-induced mono-GG Rabs were able to interact with membranes, they would not be present at the correct cellular location.

A limiting factor to mechanistic studies until now has been the relatively low affinity of 3-PEHPC, the previously reported PC inhibitor of RGGT (10). In this work, we took advantage of a newly synthesized PC derivative, (+)-3-IPEHPC, which we found to be substantially more potent (≥25-fold) than 3-PEHPC at inhibiting RGGT for all the Rab substrates that we tested. The kinetic characterization of RGGT inhibition by these PCs revealed that both compounds are uncompetitive inhibitors with respect to the Rab protein substrate and mixed-type inhibitors with respect to GGPP. We then investigated in more detail the mechanism of inhibition. Using Rab1a C-terminal mutants (CSC, CCS, CS and SC), we observed that in the presence of the singly prenylated substrates, the efficacy of inhibition was severely impaired. Moreover, the prenylation of Rab proteins with a CaaX motif (Rab13, Rab18 and Rab23) was not inhibited by (+)-3-IPEHPC. We hypothesized that only the second event of prenylation is targeted by the PCs and we verified the state of Rab1a and Rab27a prenylation after treatment with PCs. In both cases, the prenylated substrates were modified on a single cysteine, demonstrating that the inhibitors block the second addition of GGPP.

What could be the molecular basis for the inhibition of the second GG transfer? One

possibility is that the inhibitors could be interfering with the complex rearrangements that must occur on the active site of RGGT before the prenylation of the second cysteine in order to remove the first prenyl-cysteine and allow the alignment of that second cysteine with the newly bound second GGPP substrate. Interestingly, Beese and colleagues described several reaction intermediates in the FT and GGT-I reactions that allowed us to create a model for the inhibitory mechanism. These authors showed that soaking FT:prenylated peptide or GGT:prenylated peptide crystals with FPP or GGPP respectively, led to the movement of the prenylated cysteine from the active site to a new binding site in a solvent accessible groove, instead of dissociation from the enzymes (22,23). The authors further proposed that a similar process could occur in the RGGT reaction where the first GG-cysteine could be translocated to a nearby second site, allowing the second GG transfer to proceed (22). Our present studies raise the hypothesis that the PC inhibitors bind to this second site for the following reasons. First, experiments measuring the binding of GGPP to RGGT showed that the inhibitors do not preclude GGPP binding and thus suggest that the inhibitors do not bind to the GGPP-binding site. Second, the same experiments showed that the presence of inhibitor froze GGPP in its binding site suggesting that it is inhibiting GGPP transfer by preventing its movement away from the GGPP-binding site. Third, the uncompetitive kinetics vis-à-vis Rab substrates suggest that the inhibitors do not bind to the peptide-binding site.

The mechanism of RGGT inhibition by 3-PEHPC has been studied using a fluorescent analogue of GGPP (NBD-FPP) and Rab7a (ending in CXC) in a continuous fluorimetric assay (21). Strikingly, the authors observed that the use of NBD-FPP led to the formation of predominantly mono-prenylated Rab7, and not doubly-prenylated as observed using the native substrate (24). This inability of NBD-FPP to be used in the second GG addition suggests an obvious reason for the discrepancies between the studies. Furthermore, the present studies suggest that this behaviour of NBD-FPP may be related to an inability to bind the putative second site on RGGT. Recently, another study reported on the identification of novel RGGT inhibitors (25). These inhibitors appear to act via a different mechanism, probably binding to the peptide site as they exhibit competitive kinetics with respect to Rab and uncompetitive kinetics with respect to GGPP. Nevertheless, all effective inhibitors of this class required a hydrophobic tail, suggesting the possibility that binding to the putative second site may also be a feature of the inhibitory mechanism of these compounds.

Our results imply that the prenylation mechanism for singly- and doubly-prenylated Rab proteins may be different. Indeed, the prenylation of Rab5a-CVLL is not inhibited by PCs, whereas the prenylation of Rab5a-CCVLL is. The present data suggests that non-productive ESI complexes do not form in the presence of Rab-CaaX substrates, and RGGT is able to dissociate from the monoGG-Rab after prenylation. In these cases, the aaX peptide appears to be of importance because Rab1a-SC or Rab1a-CS are sensitive to inhibition, albeit at high concentrations of the inhibitors (200-fold increase compared to Rab1a WT proteins) whilst Rab-CaaX substrates are resistant. One possibility is that the aaX tail may prevent the use of the putative second site, which would allow the ready-release of the product from the enzyme. Further work will be necessary to understand the molecular basis for these differences.

Finally, we utilized the ability of PCs to inhibit the second event of prenylation to demonstrate that the N-terminal cysteine of doubly prenylated Rabs is preferred for the first event. This is in agreement with our previous report using Rab1a-CS and Rab1a-SC substrates showing that the N-terminal cysteine is more efficiently prenylated than the C-terminal cysteine (16). Moreover, it was reported the first event of Rab7 prenylation was slower than the second one (26) and the prenylation of a Rab7-SXC mutant was 3-fold faster than a Rab7-CXS mutant one (21), suggesting the N-terminal cysteine being somewhat preferred for the first prenylation event. We took advantage of the fact that Icmt can only methylate prenylated-cysteine when present at the extreme C-terminus (14,27). Here, we observed that Rab1a-CC and Rab1a-CSC substrates in the presence of inhibitor are not methylated by Icmt (Figure 6), which strongly suggests that the N-terminal cysteine of

double-cysteine containing-Rabs is preferentially prenylated.

In summary, we have characterized the mechanism of RGGT inhibition by the PC compounds, (+)-3-IPEHPC and 3-PEHPC. These inhibitors do not prevent the substrates binding to RGGT, but block the second event of prenylation possibly by binding to a second prenyl-binding site, to which the first prenyl-cysteine moves into to allow the second GG addition. Crystallisation of 3-IPEHPC:RGGT and/or 3-IPEHPC:REP:RGGT:Rab complexes should reveal this putative binding site and the reaction transition states during the complex double geranylgeranylation reaction of Rab proteins. These inhibitors might represent useful novel therapeutic agents in Rab-mediated diseases.

**References**


1. Seabra, M. C. (1998) *Cell Signal* **10**, 167-172
2. Lane, K. T., and Beese, L. S. (2006) *J Lipid Res* **47**, 681-699
3. Leung, K. F., Baron, R., and Seabra, M. C. (2006) *J Lipid Res* **47**, 467-475
4. Andres, D. A., Seabra, M. C., Brown, M. S., Armstrong, S. A., Smeland, T. E., Cremers, F. P., and Goldstein, J. L. (1993) *Cell* **73**, 1091-1099
5. Zhang, H., Seabra, M. C., and Deisenhofer, J. (2000) *Structure Fold Des* **8**, 241-251
6. Pylypenko, O., Rak, A., Reents, R., Niculae, A., Sidorovitch, V., Cioaca, M. D., Bessolitsyna, E., Thoma, N. H., Waldmann, H., Schlichting, I., Goody, R. S., and Alexandrov, K. (2003) *Mol Cell* **11**, 483-494
7. Basso, A. D., Kirschmeier, P., and Bishop, W. R. (2006) *J Lipid Res* **47**, 15-31
8. Mazieres, J., Pradines, A., and Favre, G. (2004) *Cancer Lett* **206**, 159-167
9. Coxon, F. P., Ebetino, F. H., Mules, E. H., Seabra, M. C., McKenna, C. E., and Rogers, M. J. (2005) *Bone* **37**, 349-358
10. Coxon, F. P., Helfrich, M. H., Larijani, B., Muzylak, M., Dunford, J. E., Marshall, D., McKinnon, A. D., Nesbitt, S. A., Horton, M. A., Seabra, M. C., Ebetino, F. H., and Rogers, M. J. (2001) *J Biol Chem* **276**, 48213-48222
11. Russell, R. G., Xia, Z., Dunford, J. E., Oppermann, U., Kwaasi, A., Hulley, P. A., Kavanagh, K. L., Triffitt, J. T., Lundy, M. W., Phipps, R. J., Barnett, B. L., Coxon, F. P., Rogers, M. J., Watts, N. B., and Ebetino, F. H. (2007) *Ann N Y Acad Sci* **1117**, 209-257
12. van Beek, E., Pieterman, E., Cohen, L., Lowik, C., and Papapoulos, S. (1999) *Biochem Biophys Res Commun* **255**, 491-494
13. Armstrong, S. A., Brown, M. S., Goldstein, J. L., and Seabra, M. C. (1995) *Methods Enzymol* **257**, 30-41
14. Leung, K. F., Baron, R., Ali, B. R., Magee, A. I., and Seabra, M. C. (2007) *J Biol Chem* **282**, 1487-1497
15. Seabra, M. C., and James, G. L. (1998) *Methods Mol Biol* **84**, 251-260
16. Shen, F., and Seabra, M. C. (1996) *J Biol Chem* **271**, 3692-3698
17. Gomes, A. Q., Ali, B. R., Ramalho, J. S., Godfrey, R. F., Barral, D. C., Hume, A. N., and Seabra, M. C. (2003) *Mol Biol Cell* **14**, 1882-1899
18. Seabra, M. C., Goldstein, J. L., Sudhof, T. C., and Brown, M. S. (1992) *J Biol Chem* **267**, 14497-14503
19. Desnoyers, L., and Seabra, M. C. (1998) *Proc Natl Acad Sci U S A* **95**, 12266-12270
20. Seabra, M. C., Ho, Y. K., and Anant, J. S. (1995) *J Biol Chem* **270**, 24420-24427
21. Wu, Y. W., Waldmann, H., Reents, R., Ebetino, F. H., Goody, R. S., and Alexandrov, K. (2006) *Chembiochem* **7**, 1859-1861
22. Long, S. B., Casey, P. J., and Beese, L. S. (2002) *Nature* **419**, 645-650
23. Taylor, J. S., Reid, T. S., Terry, K. L., Casey, P. J., and Beese, L. S. (2003) *Embo J* **22**, 5963-5974
24. Farnsworth, C. C., Seabra, M. C., Ericsson, L. H., Gelb, M. H., and Glomset, J. A. (1994) *Proc Natl Acad Sci U S A* **91**, 11963-11967
25. Watanabe, M., Fiji, H. D., Guo, L., Chan, L., Kinderman, S. S., Slamon, D. J., Kwon, O., and Tamanoi, F. (2008) *J Biol Chem* **283**, 9571-9579
26. Thoma, N. H., Iakovenko, A., Owen, D., Scheidig, A. S., Waldmann, H., Goody, R. S., and Alexandrov, K. (2000) *Biochemistry* **39**, 12043-12052

27. Bergo, M. O., Leung, G. K., Ambroziak, P., Otto, J. C., Casey, P. J., Gomes, A. Q., Seabra, M. C., and Young, S. G. (2001) *J Biol Chem* **276**, 5841-5845

**Footnotes**

We thank Patrick Casey for Icmt-enriched membranes and the Seabra lab for comments and helpful suggestions. Charles E. McKenna is a consultant for Procter & Gamble Pharmaceuticals. This work was supported by the Wellcome Trust (to MCS) and Procter & Gamble Pharmaceuticals (to CEMK). AT was supported by a Nuffield Foundation Studentship through the Oliver Bird Rheumatism Scheme.

**Figure legends**

**Figure 1. Inhibition of RGGT activity by phosphonocarboxylates.** Final concentrations for the reaction mix are REP1 (2μM), RGGT (50nM), GGPP (5μM), Rab1a (4μM) and increasing concentrations of (+)-3-IPEHPC (○) and 3-PEHPC (●). The reactions were incubated for 20 min at 37ºC. The values represent the means determined from duplicate determinations of two independent experiments. This experiment is representative of two other independent experiments.

**Figure 2. Characterization of the inhibition of RGGT by (+)-3-IPEHPC. (A)** Lineweaver-Burk plot for the inhibition of RGGT by (+)-3-IPEHPC when Rab1a was the varied substrate. Prenylation assays (see Experimental Procedures) were carried out in the presence of a fixed concentration of GGPP substrate (5 μM) and the indicated concentrations of Rab1a at 0 (●), 0.75 (○), or 2 μM (▼) (+)-3-IPEHPC. Data were fit to eq 1. **(B)** Lineweaver-Burk plot for the inhibition of Rab1a prenylation when GGPP was the varied substrate. RGGT assays (see above) were carried out in the presence of a fixed concentration of Rab1a substrate (4 μM) and the indicated concentrations of GGPP at 0 (●), 0.5 (○), or 1 (▼) (+)-3-IPEHPC. Data were fitted to eq 1. For both panels, data represent the means of duplicate determinations from a single experiment that is representative of three such experiments.

**Figure 3. C18 reverse-phase HPLC analysis of [$^3$H]GG-labeled Rab1a tryptic peptides.** Rabla-CC (●), Rab1a-CS (○), Rab1a-SC (▼) and Rab1a-CC + (+)-3-IPEHPC (100μM) (△) were incubated separately with [$^3$H] GGPP and RGGT/REP1, and digested with endoproteinase C-Lys. The respective digestion mixtures were then purified by reverse-phase HPLC (μRPC C2/C18 SC 2.1/10 column) using a SMART System, and the radioactivity of each fraction was plotted versus the eluted fractions. We observed similar results when the reaction mix was digested with trypsin. This experiment is representative of three independent experiments.

**Figure 4. GGPP binding to RGGT.** The prenylation mix (20μl) contains REP1 (2μM), RGGT (100nM), Rab1a (4μM) substrate, GGPP (2μM) and as indicated on the graph 100μM (+)-3-IPEHPC. After 30 min. at 37°C, 2μl of polyclonal anti-RGGT (H492) and 25μl of protein G beads were added to reaction mix and gently agitated for 2H at 4°C. The beads were washed with PBS and the immo-complexes were precipitated. GGPP molecules associated with RGGT were recovered in the supernatant and detected by scintillation counting. Background of the reaction (solution without RGGT) was removed from each observed condition. Data represent the mean of four different experiments.

**Figure 5. Prenylation and localization of GFP-Rab constructs was analyzed following transfection of 293 cells. (A)** Transfected 293 cells were treated with 0-1 mM 3-PEHPC for 18 hours, then prenylated (detergent phase; D) and unprenylated proteins (aqueous phase; A) separated by triton X-114 fractionation and GFP-Rabs detected by western blotting using an antibody to GFP. **(B)** Transfected 293 cells were

treated with (+) or without (-) 1 mM 3-PEHPC for 18 hours, then subcellular localization of GFP-Rabs assessed by confocal microscopy.

**Figure 6. Order of prenyl addition on Rab1a.** The methylation of Rab1a was measured after *in vitro* prenylation of the protein treated with (100μM) or without (+)-3-IPEHPC (for 30 min at 37ºC). 10μM of [$^3$H] S-adenosyl methionine (specific activity = 650 dpm/pmol) and 1μg of enriched Icmt membranes were added to the reaction mix for 45 min. Proteins were precipitated and the incorporated radioactivity was measured. This experiment is representative of two other independent experiments.

**Table 1: IC50 values for RGGT inhibition by (+)-3-IPEHPC and 3-PEHPC[a]**

| Rab substrate | IC50 (μM) – (+)-3-IPEHPC | IC50 (μM) – 3-PEHPC |
|---|---|---|
| Rab1a-CC (WT) | 1.27 ± 0.24 | 31.85 ± 2.13 |
| Rab1a-CSC | 1.11 ± 0.30 | ND |
| Rab1a-CS | 221.25 ± 11.49 | > 2000 |
| Rab1a-SC | 187.82 ± 8.30 | > 2000 |
| Rab1a-CCS | 0.91 ± 0.25 | ND |
| Rab27a-CGC (WT) | 0.83 ± 0.50 | 32.68 ± 1.95 |
| Rab27a-CVLS | > 800 | > 2000 |
| Rab5a-CCSN (WT) | 0.43 ± 0.06 | 43.47 ± 9.85 |
| Rab5a-CCQNI | 16.52 ± 4.42 | > 2000 |
| Rab5a-CCVLL | 5.91 ± 0.50 | 860 ± 80 |
| Rab5a-CVLL | > 800 | > 2000 |
| Rab6a-CSC | 27.22 ± 2.28 | 1592 ± 95 |
| Rab13-CSLG (WT) | > 800 | > 2000 |
| Rab18-CSVL (WT) | > 800 | > 2000 |
| Rab23-CSVP (WT) | > 800 | > 2000 |

a The values represent the means ± the standard error of the mean determined from duplicate determinations of at least two independent experiments.

**Table 2: Experimental kinetic constants for RGGT inhibition by (+)-3-IPEHPC and 3-PEHPC[a]**

| | **Substrate** | |
|---|---|---|
| **Inhibitor** | **Rab1a** | **GGPP** |
| **(+)-3-IPEHPC** | Uncompetitive<br>Ki = 0.211 ± 0.091 μM | Mixed-type<br>Ki = 0.074 ± 0.029 μM |
| **3-PEHPC** | Uncompetitive<br>Ki = 33.56 ± 11.05 μM | Mixed-type<br>Ki = 5 ± 0.18 μM |

[a] The values represent the means ± the standard error of the mean determined from duplicate determinations of three independent experiments.

Figure 1

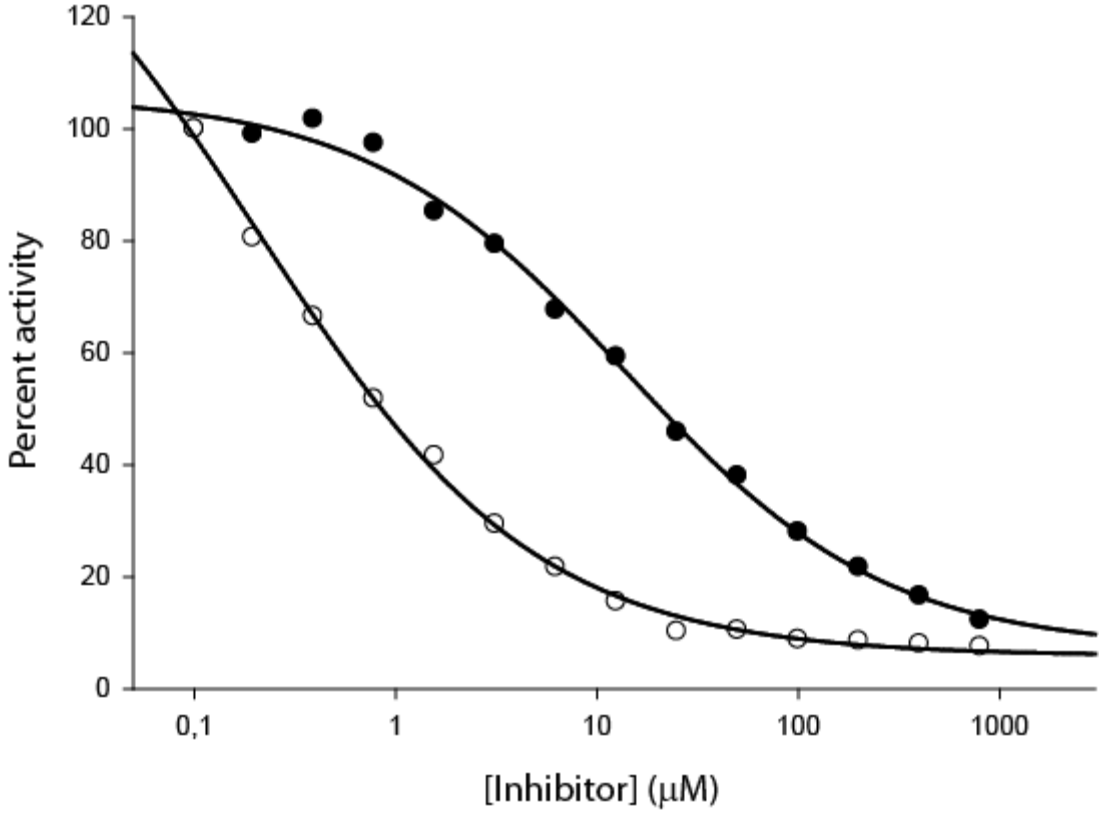
120
100
80
60
40
20
0
Percent activity
0,1
1
10
100
1000
[Inhibitor] (μM)

Figure 2A

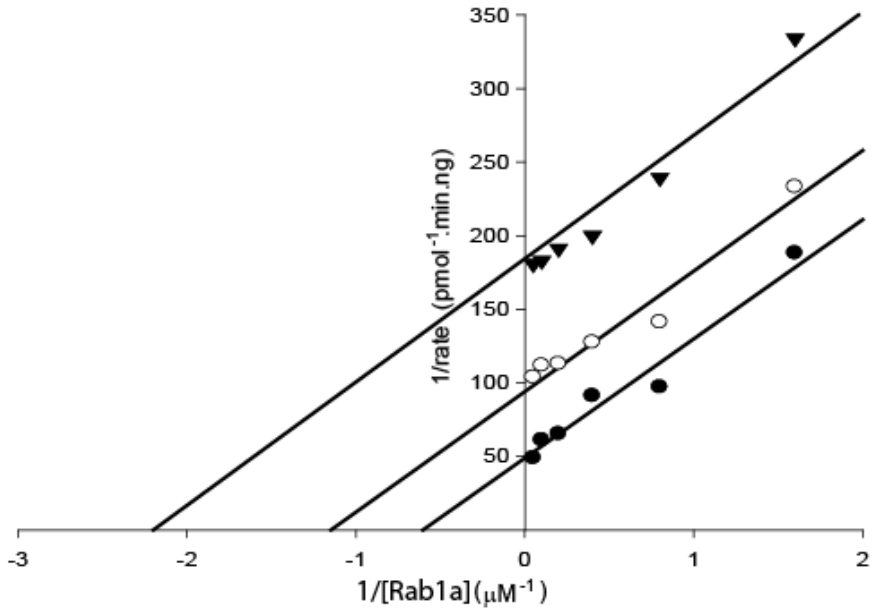


Figure 2B

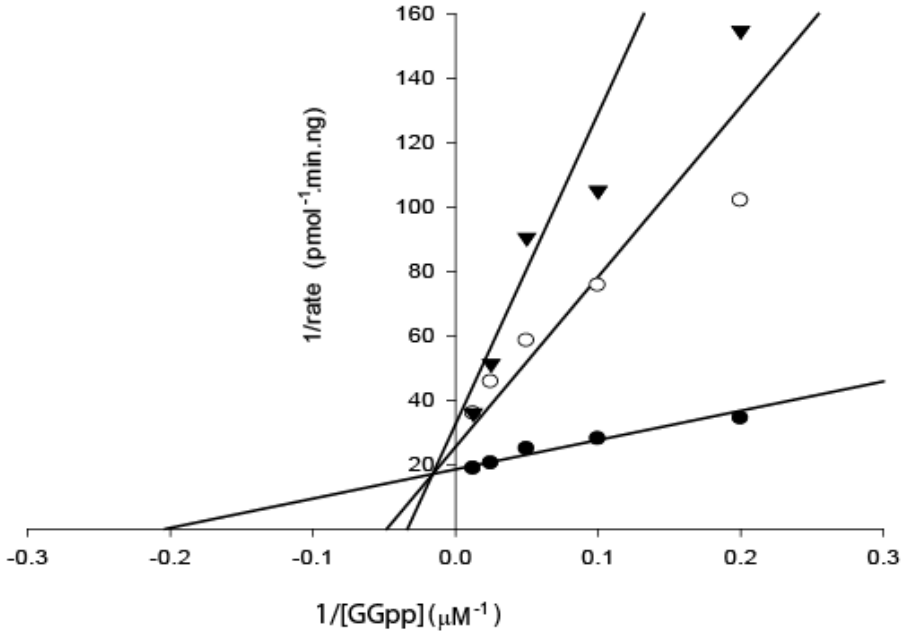

Figure 3.

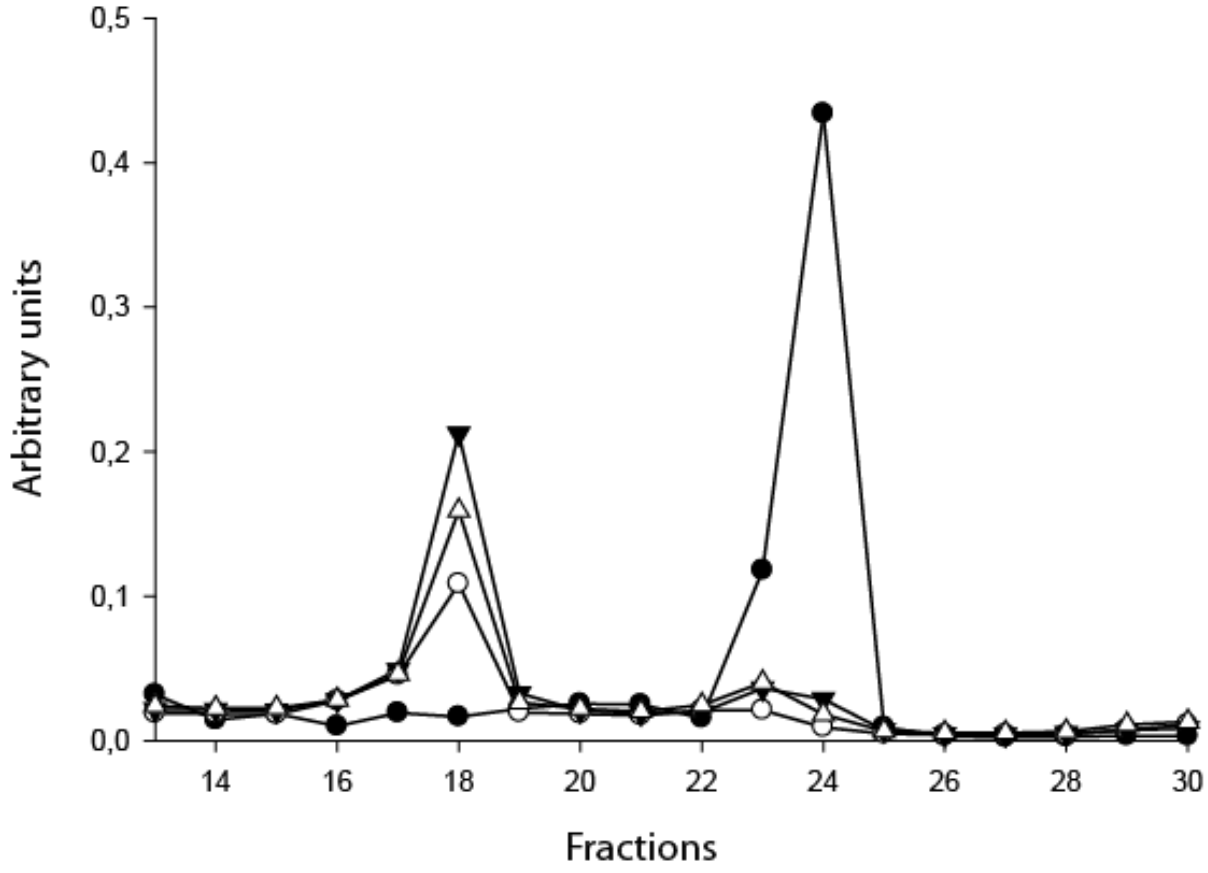
0,5
0,4
0,3
0,2
0,1
0,0
Arbitrary units
14
16
18
20
22
24
26
28
30
Fractions

Figure 4

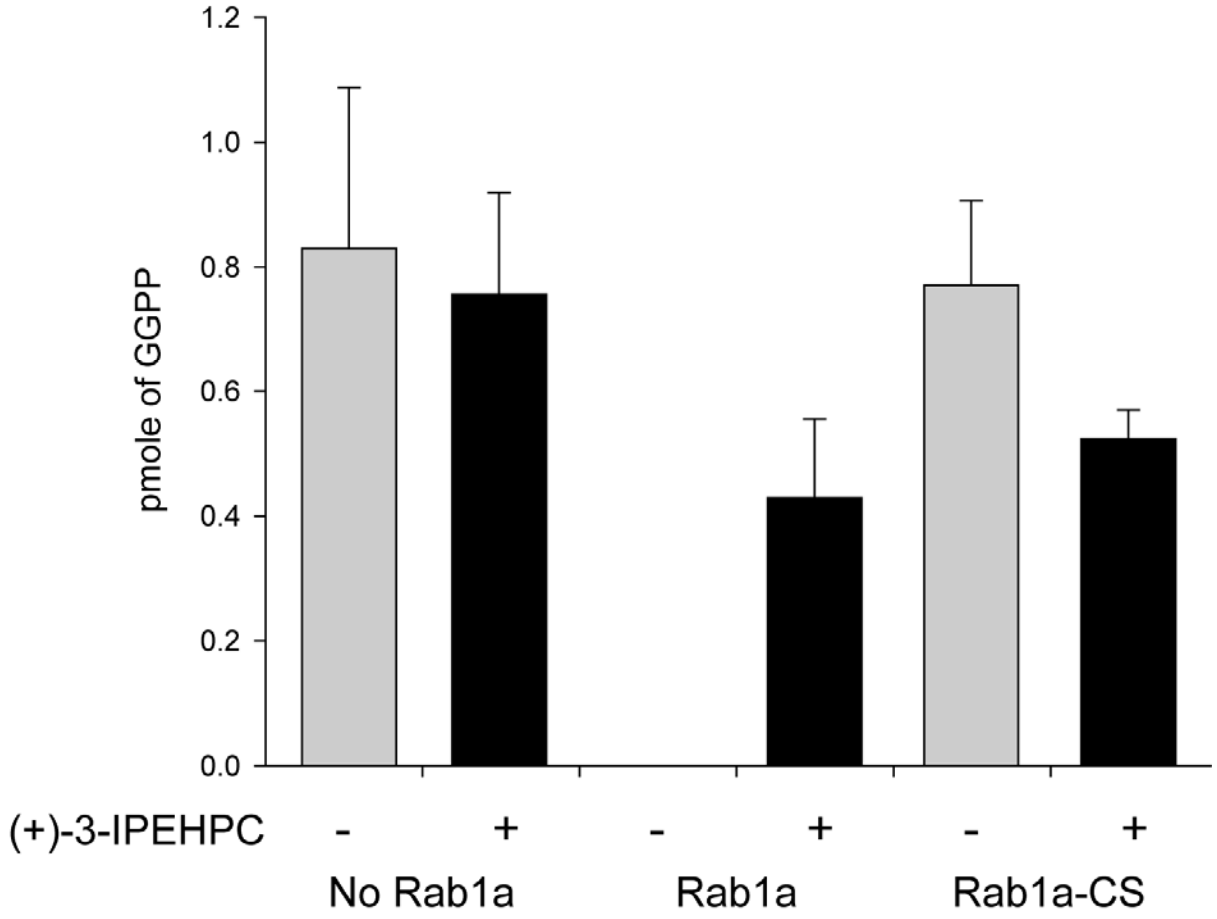
1.2
1.0
0.8
0.6
0.4
0.2
0.0
pmole of GGPP
(+)-3-IPEHPC
-
+
-
+
-
+
No Rab1a
Rab1a
Rab1a-CS

# Figure 5

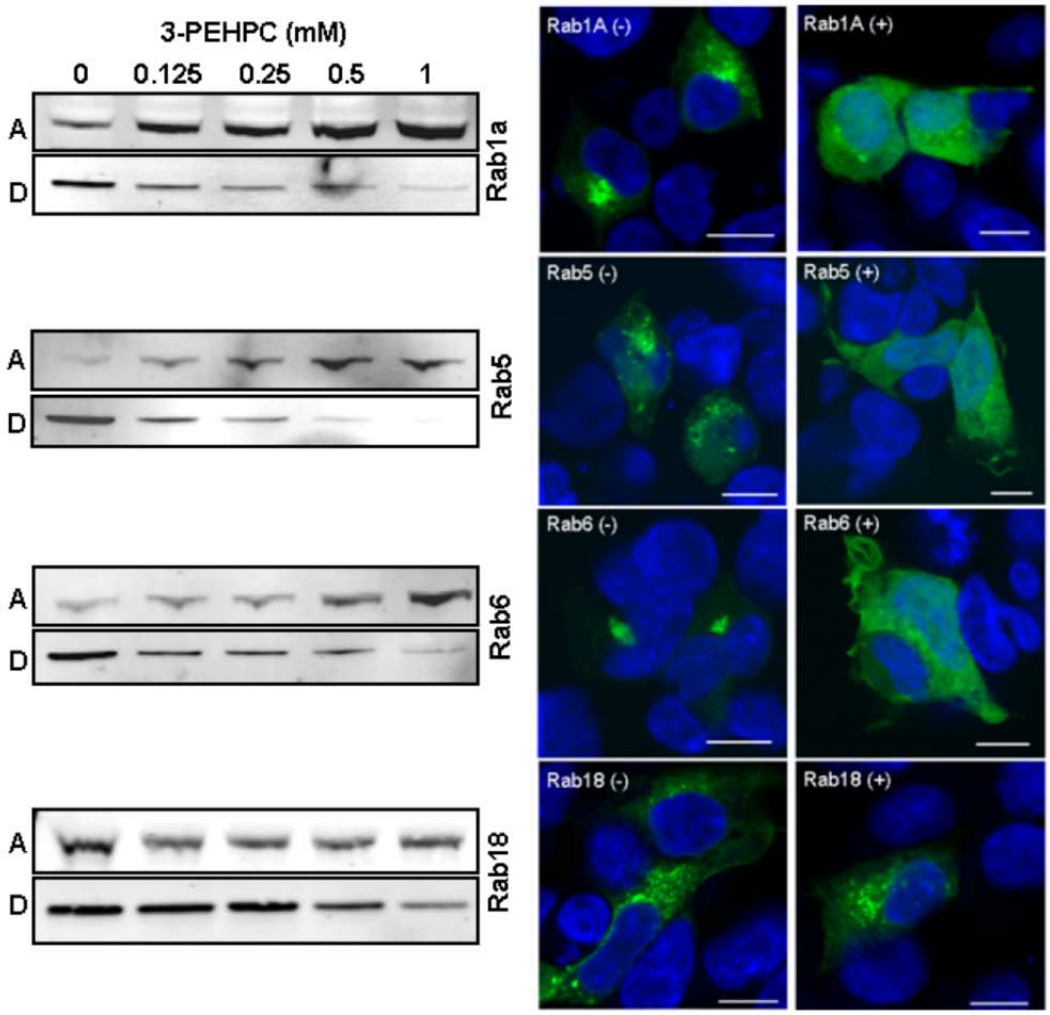
3-PEHPC (mM)
0
0.125
0.25
0.5
1
A
D
Rab1a
Rab5
Rab6
Rab18
Rab1A (-)
Rab1A (+)
Rab5 (-)
Rab5 (+)
Rab6 (-)
Rab6 (+)
Rab18 (-)
Rab18 (+)

Figure 6

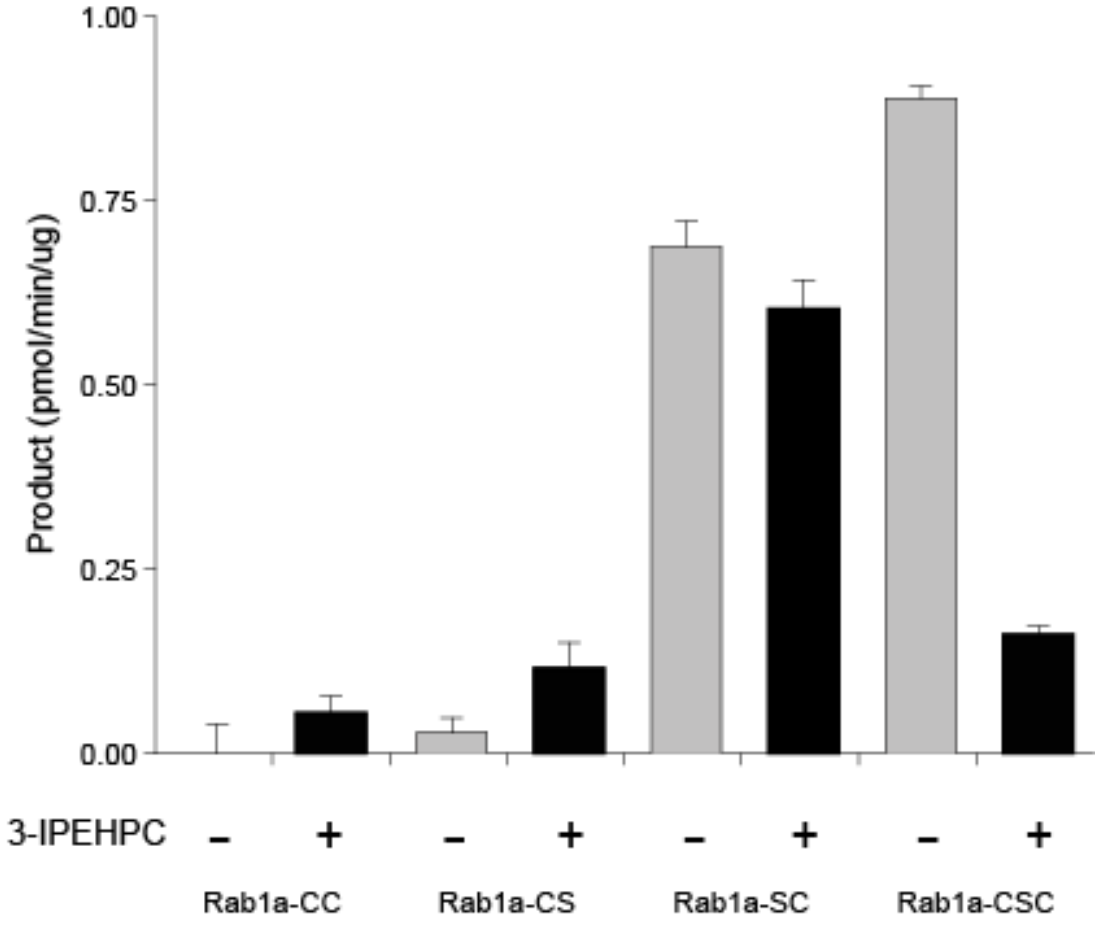
1.00
0.75
0.50
0.25
0.00
Product (pmol/min/ug)
3-IPEHPC
–
+
–
+
–
+
–
+
Rab1a-CC
Rab1a-CS
Rab1a-SC
Rab1a-CSC